J. Membrane Biol. 3, 180–209 (1970)

Electrical Activity and Metabolism in Cardiac Tissue: An Experimental and Theoretical Study

H. G. HAAS, R. KERN, and H. M. EINWÄCHTER

First Department of Physiology, University of Heidelberg, Heidelberg, Germany

Received 10 April 1970

Summary. (1) Effects of the metabolic inhibitor 2,4-dinitrophenol (DNP) on electrical activity in frog atria were studied by means of the sucrose-gap technique and in tracer experiments. (2) Voltage-clamp studies of ionic membrane currents showed a suppression by DNP of peak Na inward current without marked changes in the kinetics of the Na-carrying system and an increase of steady state outward current to three to five times its normal value. In ^{42}K tracer experiments, DNP increased K resting efflux by about 10% and decreased K influx by 25 to 30%. (3) The depression of Na inward current is regarded as being caused by a partial block of Na channels and an increase of internal Na concentration after inhibition of active Na extrusion. (4) The strong rise in outward current is probably not caused by a K current since K efflux fails to show a correspondingly large change. As a possible explanation for current and flux changes, an electrogenic K pump is discussed. (5) A mathematical model of a carrier system transporting a single ion species is described. The system is designed as a direct "potential" pump. Uphill transport requires an asymmetry of the rate constants governing the cyclic formation and breakdown of carrier-ion complex. The asymmetry is brought about by an input of metabolic energy. Reduction of energy input decreases the asymmetry and induces a carrier-mediated downhill ion movement, with corresponding changes in membrane current and ion fluxes. (6) A model of electrogenic K inward transport is calculated that approximately accounts for the steady state current and the K flux changes experimentally observed after inhibition.

It has long been known that electrical activity of the heart is closely related to cell metabolism. Unlike nerve (Hodgkin & Keynes, 1955*a*, *b*), cardiac tissue exhibits marked changes in the shape of the action potential when the utilization of metabolic energy is reduced by anoxia, fatigue, enzyme inhibitors, or similar factors. The most prominent change associated with a metabolic inhibition is a shortening of the action potential caused by an accelerated repolarization. Concomitantly, a reduced amplitude and a raised threshold of the action potential and a depolarization of the resting potential may be observed. Despite a number of investigations (Trautwein & Dudel, 1956; Webb & Hollander, 1956; Lüllmann, 1959;

Macfarlane, 1960; Kleinfeld, Magin & Stein, 1961; Haas, Hantsch, Otter & Siegel, 1967), there is no generally acceptable idea of the pattern of interplay between metabolism and the ionic movements underlying the cardiac action potential. The main concepts proposed are the presence of energy-dependent structures controlling ionic permeabilities of the membrane, an active ion transport across the membrane maintaining the concentration gradients for passive ion movements, and a direct contribution of active transport to membrane current in the form of an electrogenic pump. The latter concept is particularly attractive for an interpretation of the plateau of the normal action potential and the loss of plateau owing to inhibition (Brady & Woodbury, 1951; Macfarlane, 1960).

In this paper, the problem of interaction between electrical activity and metabolism is treated on the basis of voltage-clamp studies and flux measurements in frog atria. 2,4-Dinitrophenol (DNP) was employed as inhibiting agent. Using the sucrose-gap technique, the influence of inhibition on membrane currents was tested. DNP was found to strongly reduce peak Na inward current whereas the kinetics of activation, inactivation, and reactivation of the Na-carrying system was little affected. The reduction in magnitude may be explained by an alteration of membrane structure resulting in a decreased number of available Na channels and by inhibition of active Na extrusion leading to a decreased Na concentration gradient. On the other hand, steady state outward current was greatly augmented by application of DNP. If steady state current is interpreted as passive movement of K ions, an increase of K membrane conductance by 200 to 400% must be assumed for a given membrane potential. This assumption, however, is inconsistent with ^{42}K flux measurements which showed that K resting efflux increased by not more than 10 to 15% and that K influx decreased by about 25% after inhibition. As an alternative, we examined the possibility that the changes in steady state current and K fluxes could be attributed to inhibition of an electrogenic K pump.

The Appendix of this paper presents a quantitative theoretical treatment of a membrane carrier system transporting ions uphill. Transport is understood to be a net movement involving a unidirectional influx and efflux. The system is designed to have affinity to one particular cation species only. The free and loaded carriers are taken as anion and electroneutral molecule, respectively. Owing to the movement of free carrier, the system is directly involved in electrical membrane phenomena. With given values of the kinetic parameters, ion transport can be determined as a function of membrane potential. A block of energy supply owing to inhibition causes the system to perform a downhill movement rather than an uphill transport,

thus inducing definite changes in membrane current and fluxes. A model of electrogenic K inward transport is numerically calculated for membrane potentials between -100 and $+105$ mV. Simulating an inhibition yields a decrease of carrier-mediated K influx as well as an increase of K efflux, both effects resulting in an increase of outward current. With use of proper values for the parameters of the system, a fair correspondence between theoretical and experimental data is obtained. There is no need to assume a change in the passive properties of the membrane. The strong increase in membrane current is explained by the assumption that in normal preparations a large part of passive K outward current is counterbalanced by electrogenic inward transport. Thus a small change in carrier-mediated fluxes owing to inhibition will lead to a large change in net membrane current.

Materials and Methods

Solutions

Ringer's solution of the following composition was used as bathing and perfusing fluid: 111 mM NaCl, 5.4 mM KCl, 1.8 mM $NaHCO_3$, and 1.8 mM $CaCl_2$. The test solution was obtained by adding 0.5 mM DNP to 1 liter of Ringer's fluid. The pH was adjusted to a value between 6.9 and 7.1. Isosmotic KCl solution was 121 mM and isosmotic sucrose solution was 242 mM. Ringer's fluid, test solution, and KCl solution were bubbled with a gas mixture of 95% O_2 and 5% CO_2 throughout the experiments. For tracer experiments, a ^{42}K Ringer's fluid with a specific activity of about 1 mC/mg K was used as "active bath".

Experimental Arrangement

Voltage-clamp measurements were made using a modification of the sucrose-gap technique of Julian, Moore and Goldman (1962*a*, *b*). Fig. 1 illustrates the arrangement. A thin bundle of atrial tissue (diameter about 0.3 mm, length between 6 and 8 mm) from a bullfrog heart was mounted in a Plexiglas chamber so that a short segment (about 0.2 mm in length) in the middle of the preparation was electrically isolated from the ends by two streams of isosmotic sucrose solution filling the extracellular space. The gap between the two sucrose streams was perfused by Ringer's fluid or by the test solution. The ends of the preparation were in side pools containing isosmotic KCl solution. Side pools and gap were freely accessible from the surface. Through the high (about 20 MΩ) extracellular resistance of the sucrose streams, a current could be injected from one side pool to the gap, and the membrane potential within the gap could be measured with respect to the other side pool by extracellular Ag–AgCl electrodes. By connecting the electrodes to a feedback amplifier (with an open loop gain of 10^8 or more), a voltage-clamp circuit was established. Starting from a holding potential (*HP*) near the resting value, the membrane potential was displaced in rectangular steps and the associated membrane currents were measured. At the beginning and the end of a step, full control of the membrane potential was reached in less than 500 μsec. Owing to the smallness of the gap, an approximative uniformity of membrane potential and membrane current in the central segment is to be expected. To clarify this point, we

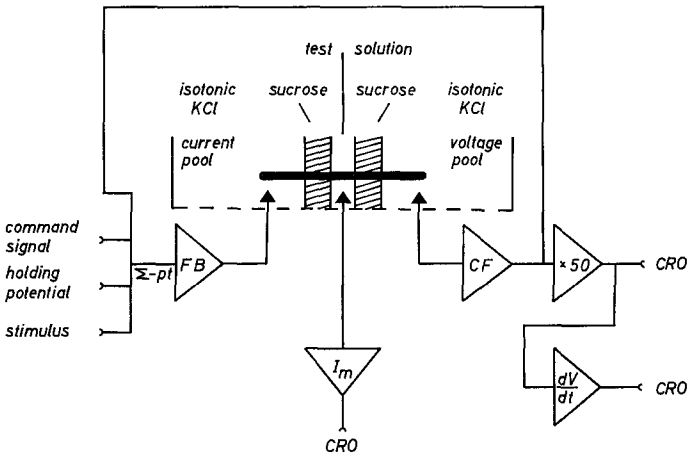

Fig. 1. Schematic diagram of the voltage-clamp circuit. The preparation is shown as a black strip. Electrodes are represented by small filled triangles. A reference electrode in the central pool which was used in potential measurements is omitted. The current electrode in the central pool is virtually grounded. A Bak amplifier (Bak, 1958) was used as cathode follower (*CF*). All other amplifiers were operational amplifiers used in a potentiometric or in a currentometric feedback configuration (*FB*, control amplifier; I_m, membrane current measurement)

checked, in preliminary experiments, the membrane potential at various points of the gap by internal microelectrodes which were completely separated from the voltage-clamp circuit. These measurements showed that, during a superthreshold clamp, the spatial variation of the membrane potential within the gap was less than 2 mV in the phase of initial inward current and almost zero in the later phases. Furthermore, the microelectrode measurements showed that there was no serious distortion of the clamp by an extracellular resistance (*see* Beeler & Reuter, 1970). When a rectangular step depolarization was indicated by the external Ag–AgCl electrodes, the potential change recorded between the internal microelectrode and a nearby reference microelectrode was almost the same, except for a small hump (up to 5 mV) at the peak of a large inward current. The membrane current was measured in its absolute value (μA). It refers to a volume of cells in the order of 0.01 mm^3. Because of the complexity of myocardial structure, no attempt was made to determine current density. Assuming cylindrical cells of 4-μ diameter, the scaling factor for converting volume data into surface data would be 10^3 mm^{-1} (Haas & Glitsch, 1962).

^{42}K flux measurements were performed with the usual technique (Haas *et al.*, 1967). Resting frog atria (after removal of pacemaker tissue) were used as preparations. For a determination of K influx, the preparation was soaked in ^{42}K-labelled Ringer's solution for a few minutes, and the radioactivity taken up was measured by a γ-scintillation counter. Assuming a complete exchange between the soaking-in solution and the extracellular space (which was taken as 35% of the wet weight of the preparation), ^{42}K uptake of the cells was calculated by an appropriate subtraction from the ^{42}K uptake of the preparation. K influx through the cell membrane was obtained by dividing ^{42}K uptake by the weight of the cells and the duration of the soaking-in period. For K efflux measurements, the preparation was loaded with ^{42}K over 3 to 4 hr and then transferred

through a series of test tubes containing inactive Ringer's fluid. From the radioactivity released into the test tubes per minute and the residual activity of the preparation, the rate constant of K efflux was determined.

Temperature

All experiments were done at 4 to 7 °C.

Nomenclature

The value of absolute membrane potential (inside negative) is denoted by E. A positive shift in membrane potential means a depolarization, a negative shift a hyperpolarization. Thermodynamic equilibrium potentials as calculated from the Nernst equation are denoted by E_{Na}, E_K, etc. Ionic membrane current I and its components I_{Na}, I_K, etc., are positive when equivalent to an outward flow of cations. Intracellular and extracellular ion concentrations (strictly speaking, activities) are designated by the subscripts i and o, respectively.

Results

Resting Potential and Action Potential

With normal Ringer's fluid perfusing the gap, the resting potential of 23 preparations was found to range between -65 and -82 mV (mean -72 mV, SE ± 4 mV). The resting potential in the sucrose gap was distinctly higher than that measured with an internal microelectrode in the absence of sucrose: -63.4 ± 4 mV (mean $\pm$SE; *see* Haas *et al.*, 1967). This hyperpolarization is similar to that observed on lobster and squid axons (Julian *et al.*, 1962*a*, *b*; Narahashi, Moore & Scott, 1964). According to Stämpfli (1963) and Blaustein and Goldman (1966), the hyperpolarization is due to a liquid junction potential at the sucrose-Ringer boundary.

When 0.5 mM DNP was added to the perfusing fluid, the resting potential underwent a transient hyperpolarization of 2 to 5 mV, which was maximal after about 8 min, and then a slow depolarization up to 7 mV after 25 min. The action potential (Fig. 2) showed a gradual decrease in rate of rise and height as an early finding starting after about 3 min of exposure and combined with an increasing threshold. In some preparations, we observed a transient prolongation of the action potential in the beginning of the DNP period (Fig. 2a). After about 10 min, a loss of plateau became evident (Fig. 2d), resulting in a progressive shortening of the action potential. After 15 to 20 min, regenerative activity was blocked. Washing in normal Ringer's fluid led to a partial recovery of the action potential unless the duration of the DNP period was longer than 25 min.

The observation that DNP affected the rising phase of the action potential earlier than the plateau was somewhat unexpected since previous work

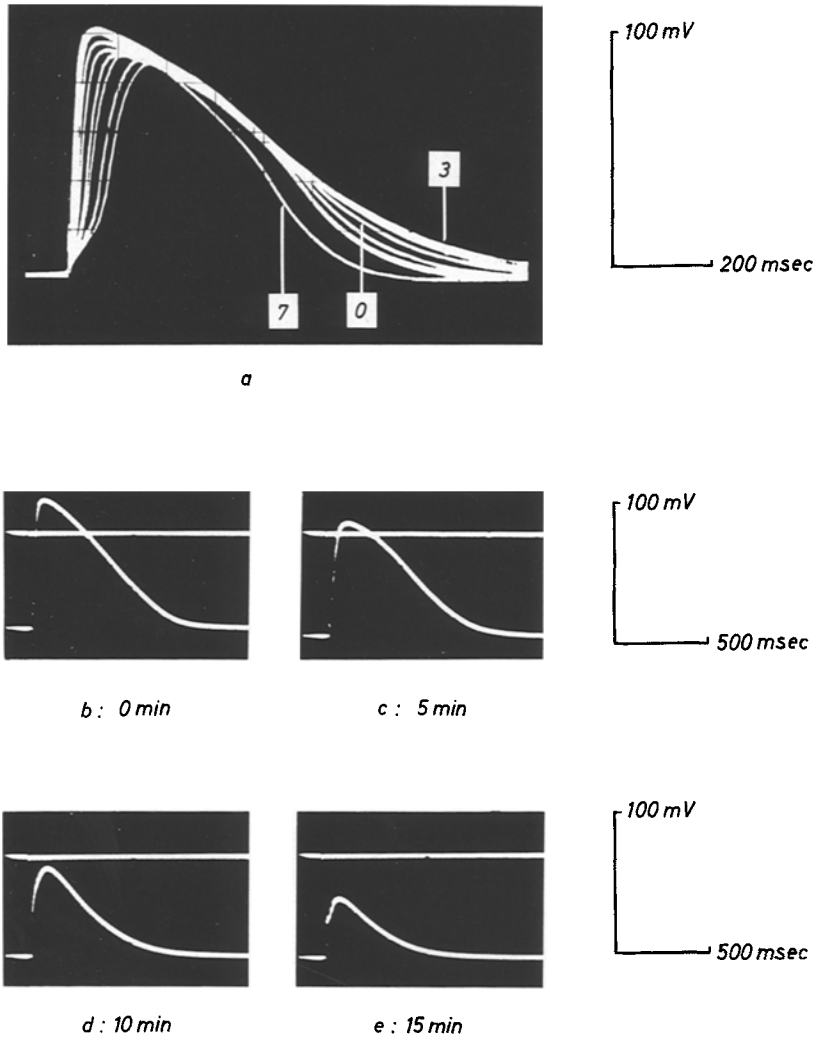

Fig. 2a–e. Influence of DNP on frog atrial action potential. (a) Superimposed traces of action potentials recorded during exposure to DNP for 7 min. Records in normal Ringer and after 3 and 7 min of exposure to DNP are indicated by 0, 3, and 7. No marked change of the resting potential is seen. (b)–(e) Single records from another strip after various times of exposure to DNP. Note a small hyperpolarization of the resting potential in (c)

had shown a loss of plateau as the first effect (Haas *et al.*, 1967). This difference in the sequence of events may be explained by a difference in temperature which was 21 to 23 °C in the earlier experiments and 5 °C in the measurements presented here.

Membrane Currents during Voltage Clamp

The membrane current associated with a superthreshold depolarizing clamp consists typically of a short capacitive surge at the make and break of the pulse and the ionic currents flowing across the membrane during the pulse; namely, (1) a fast initial wave of inward (Na) current, (2) a slow inward current, probably carried by Na and/or Ca ions (Rougier, Vassort, Garnier, Gargouil & Coraboeuf, 1969) with a threshold at about −20 mV, and (3) a slow outward current approaching a steady state after 100 to 200 msec. Since the slow inward current varies considerably in different preparations, attention has been focused on the fast inward and the slow outward currents.

Fig. 3a shows a family of curves representing fast initial inward current in normal Ringer's fluid at various levels of depolarization. Threshold was found at a membrane potential between −50 and −40 mV. The general configuration of transient inward current was similar to that observed in squid axon, except that the time course of activation and inactivation was somewhat slower. The amplitude of inward current had a maximum at a clamped potential of −30 mV and decreased with greater depolarization. A conversion from inward to outward current as was expected at strong depolarizations was not seen. Probably it was obscured by large capacity currents.

Application of DNP caused a drastic depression of fast inward currents. Fig. 3b illustrates the time course of the decrease of inward current at a given voltage. Within 15 min, inward current was reduced to about 1/10 of its original value. There was no marked shift in the time between the onset of the pulse and the peak of inward current, and the time course of inactivation was almost unchanged. After the preparation was returned to normal Ringer's fluid, a fast but incomplete recovery of transient inward current was observed. The influence of DNP on the process of reactivation of fast inward current was tested using the double-pulse arrangement proposed by Hodgkin and Huxley (1952*a*). Fig. 4a shows an experiment in normal Ringer's fluid. Two short rectangular pulses were applied in succession, and the amplitudes of the corresponding inward currents were compared. For intervals longer than 800 msec, the two inward currents were identical. With decreasing intervals, the second inward current was progressively reduced owing to a residual of inactivation of the Na-carrying system caused by the first pulse. By plotting the peak of the second inward current against the duration of the interval, a time constant of 115 msec was found for the removal of inactivation after the first pulse. Fig. 4b

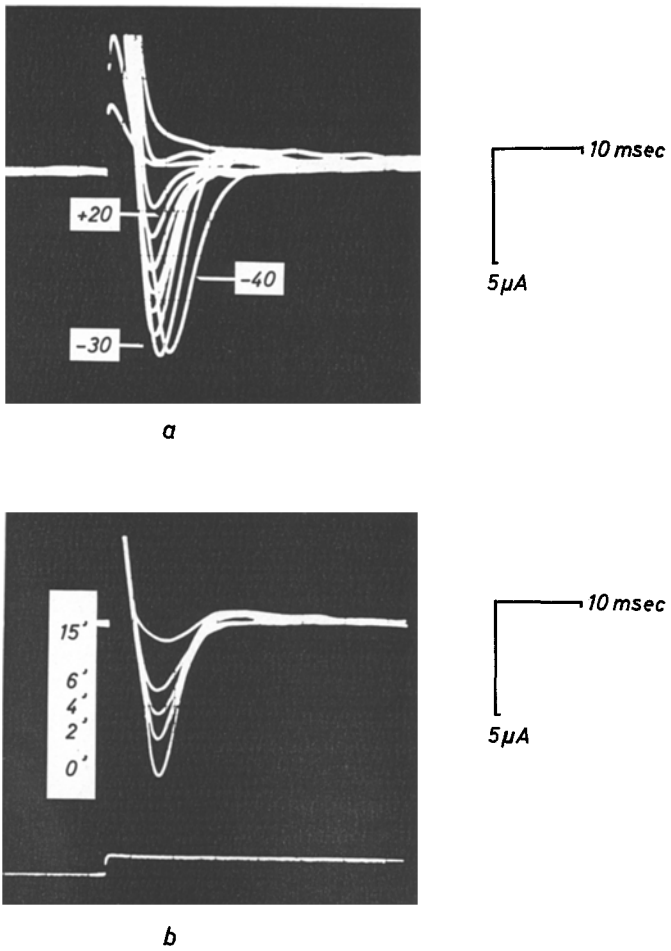

Fig. 3a and b. Initial inward currents observed with voltage clamps. In this and the following figures, inward current is shown as a downward deflection. (a) Superimposed records obtained in normal Ringer's. The membrane was depolarized in 10-mV steps ranging from 10 to 110 mV. The holding potential was −60 mV. For three curves, the value of the absolute membrane potential during the pulse is indicated. The 10-mV step was below threshold whereas the 20-mV step caused a large inward current. Activation of inward current was overlapped to some extent by the capacity current associated with the onset of the clamp. Inactivation was found to be a simple exponential decay with time constants between 2.9 and 4.2 msec. (b) Suppression by DNP of inward current at a fixed step depolarization of 40 mV. *Upper beam*: Superimposed traces of inward current. Times (in min) of exposure to DNP are given beside the peaks. *Lower beam*: Membrane potential

shows the analogous experiment carried out after initial inward current had been suppressed to about 1/2 by application of DNP. The time course of reactivation appears somewhat slowed. However, using the single records

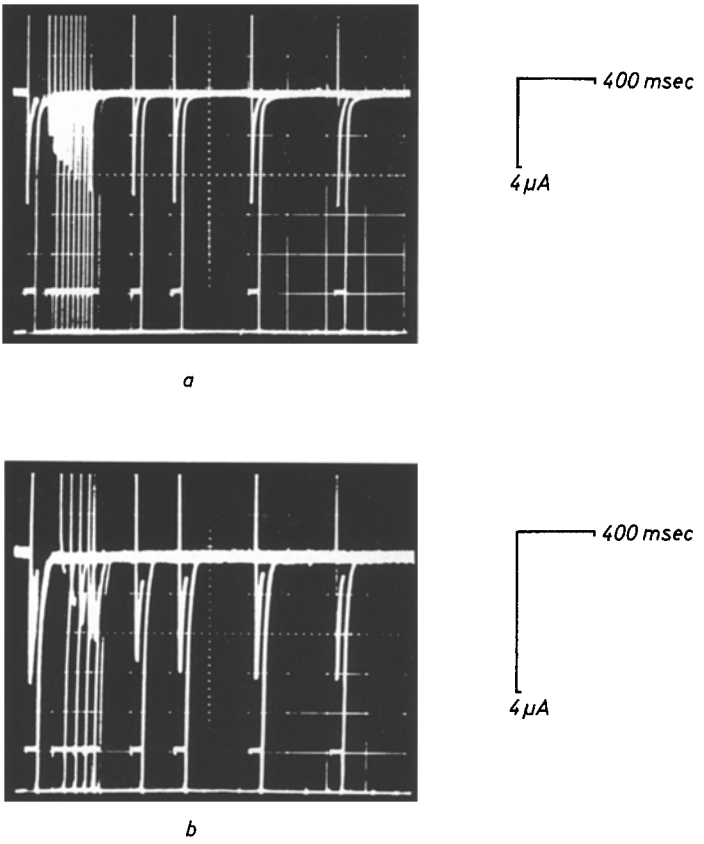

Fig. 4a and b. Recovery of fast inward current from inactivation measured with two consecutive depolarizing pulses of 50-mV amplitude and 52-msec duration. Superimposed traces of membrane current (upper beam) and voltage (lower beam). $HP = -70$ mV. The first pulse is shown at the extreme left; the second pulse is initiated at various times after the cessation of the first one. The vertical bars limited by the upper and lower edge are the capacity currents at the making and breaking of each pulse. Fast inward current is a short spike. The pulse duration is long enough for the inward current to be inactivated almost completely during the first pulse. (a) Reactivation in normal Ringer's. (b) After 5 min of exposure to DNP, the time course of reactivation is little affected. Same preparation as in (a). Note that the current scale has been doubled

instead of the superimposed traces revealed that peak inward current associated with the first pulse declined by about 10% between the first record (with the smallest interval between the two pulses) and the last one (with the largest interval). If a correction is made for this progressive change, the time constant of reactivation is almost the same as in the controls.

To investigate the slow component of membrane current, long pulses of about 1-sec duration were used. Fig. 5a shows a family of curves recorded

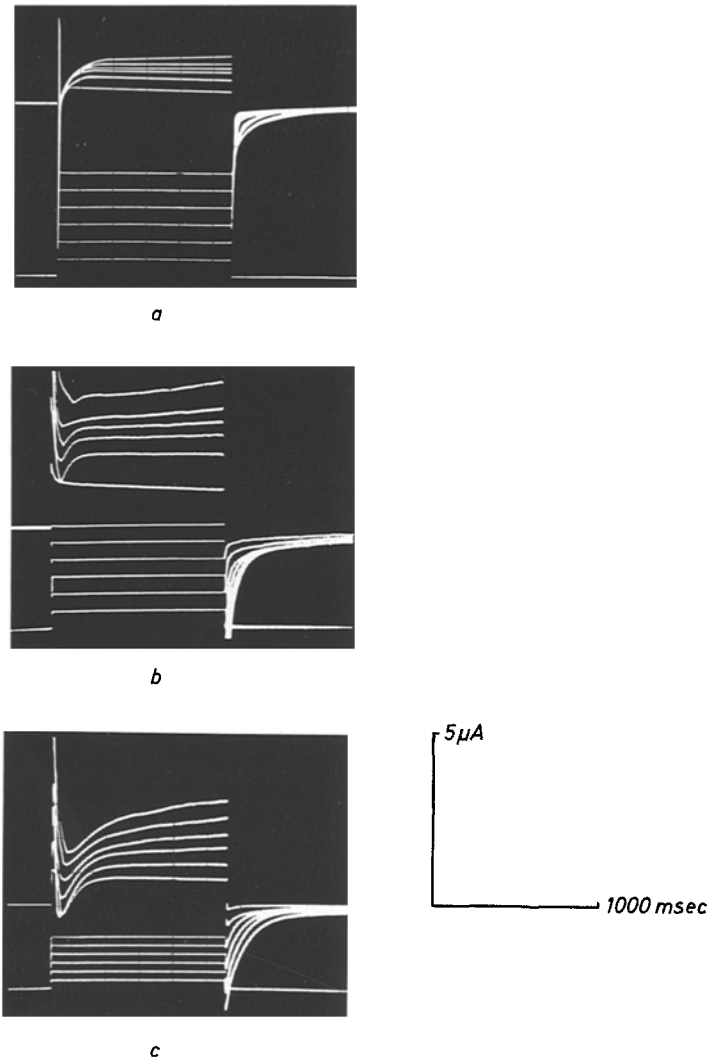

Fig. 5a–c. Families of membrane currents (upper traces) associated with long step depolarizations (lower traces) in (a) normal frog atria, (b) those treated with DNP for 15 min, and (c) those recovering from DNP for 10 min. $HP = -80$ mV. Membrane potential is displaced in 20-mV steps (a & b) and in 10-mV steps (c). In (b) and (c), outward current is greatly augmented in all steps; at strong depolarizations, steady state is not yet reached at the end of the pulse. In the controls, initial inward current is seen as a very short spike. In (b) and (c), small downward deflections represent the residual inward current. An apparent prolongation of the time to peak may be due to an overlapping of decreased inward and increased outward current

in normal Ringer's fluid. The fast initial inward current was barely visible at the slow sweep speed used. It was followed by a long-lasting outward current which rose as a function of time and attained an approximative

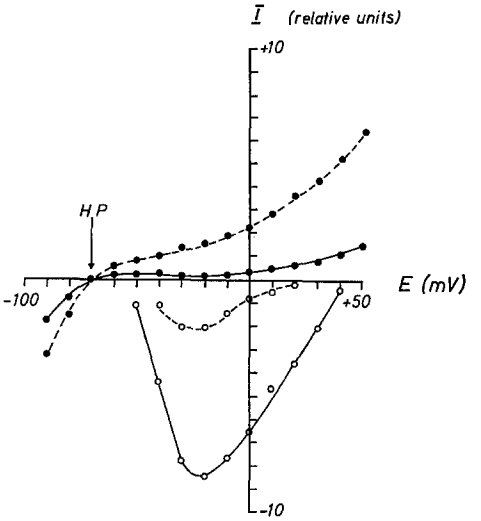

Fig. 6. Current-voltage relations for peak transient inward current (○) and steady-state current (●) in normal frog atria (full lines) and those treated with DNP (broken lines). Average values of membrane current from eight preparations (after correction for differences in bundle diameter). Decrease of inward current and increase of steady state current were measured after 8 and 15 min of exposure to DNP, respectively

steady state level after 100 to 200 msec. At depolarizations stronger than 100 mV, there was a slow increase of outward current over the whole duration of the clamp. In this range of potential, pulses of about 3-sec duration were needed to establish a true steady state of outward current. Fig. 5b illustrates the effect of DNP. In contrast to the strong depression of inward current, slow outward current greatly increased during exposure to DNP. After 15 min, an increment of 200% or more was observed at any level of depolarization. An increase was also found for steady state inward currents associated with hyperpolarizing clamps. Increase of steady state current started later than decrease of transient inward current and did not reach a maximum within 20 min. After washing with normal Ringer's fluid (Fig. 5c), steady state current continued to rise whereas initial inward current showed a partial recovery.

Fig. 6 summarizes the results of eight experiments with clamped potentials between −90 and +50 mV. The graph is a plot of the current-voltage relation for peak initial inward current and steady state current before and during application of DNP. The suppression of transient inward current and the enhancement of steady state current is clearly seen. The intercept of the curve representing normal peak inward current with the abscissa a

$E = +42$ mV roughly corresponds to the Na equilibrium potential E_{Na} (Haas, Glitsch & Trautwein, 1963). After treatment with DNP, there is an apparent shift of E_{Na} to lower values of membrane potential, but because of the asymptotic nature of the Na curve it is hard to say what the exact value of E_{Na} is. Normal steady state current exhibits a strong "anomalous" (inward-going) rectification. After application of DNP, anomalous rectification is still present but attenuated. The zero point of steady state current has the same location on the voltage axis (-70 mV) in the controls and in the measurements with DNP, according to the fact that there is no appreciable change in the resting potential after 15 min of exposure to DNP (*see* Fig. 2).

^{42}K *Fluxes*

For K influx measurements, two ^{42}K-labelled soaking-in solutions were used which were identical in composition except that one solution contained 0.5 mM DNP. Fifty quiescent frog atria were soaked in each solution for 5 min, and resting influx per kg cells (wet weight) and per min was calculated from the quantity of labelled K taken up. Since electrical measurements had shown a delay in the action of DNP, the preparations which were immersed in the DNP-containing bath had been pretreated with inactive DNP-Ringer's for 10 min. The control value of K influx came to 1.4 ± 0.3 mM/kg min (mean $\pm$SE). In the preparations bathed in the DNP-containing solution, K influx was 1.0 ± 0.2 mM/kg min (mean $\pm$SE). This means a reduction by DNP of K influx by about 29%.

K efflux was measured in preparations which had been equilibrated with ^{42}K. By transferring the preparation through 30 test tubes filled with inactive Ringer's fluid (1 min in each tube), the fraction of ^{42}K lost per min (the rate constant k) was determined. This procedure was performed on 40 preparations – 20 controls and 20 experiments in which DNP was added to the inactive Ringer's fluid between the 11th and 25th minute. The mean values of k as a function of time are shown in Fig. 7. In normal Ringer's fluid, the k values decrease continuously during the first 10 min (probably because of a wash-out of extracellular ^{42}K) and then reach an approximately constant level which is representative for the release of intracellular ^{42}K (*see* Haas *et al.*, 1967). In this stage, the rate constant is a relative measure of K efflux and any change in efflux is reflected by a corresponding change in k. The effect of DNP on ^{42}K release is to raise the rate constants by about 10% compared to the controls. This is equivalent to a rise of K efflux by the same percentage. Because of the smallness of this effect, it is hard to say how it develops with time.

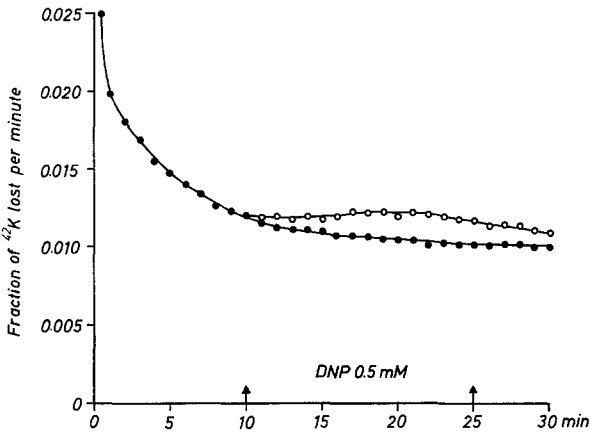

Fig. 7. Effect of DNP on K efflux. Abscissa: Time after the beginning of the washing-ou process. Ordinate: Fraction of ^{42}K lost per min in controls (•) and during applicatio of DNP (○). Mean values from 40 experiments

Discussion

To begin with, a qualitative conformity between the DNP-induce changes of the action potential and the voltage-clamp data can be stated The decreased rate of rise and amplitude and the accelerated repolarizatio of the action potential are obviously correlated to the reduction by DNI of transient inward current and the increase of slow outward current.

There is good evidence that fast initial inward current in frog atria i mainly carried by Na ions: (1) its kinetics is very similar to that in nerve and (2) it is almost completely suppressed by low concentrations of tetro dotoxin and by removal of Na from the external solution (Rougier, Vassor & Stämpfli, 1968). By contrast, the exact nature of slow outward curren in cardiac tissue is far from clear. Apart from K ions, Na, Cl, and Ca ion and an unknown ion species have been suggested to be involved in the slo current flowing during a depolarization (Deck & Trautwein, 1964; Traut wein, Dudel & Peper, 1965; Dudel, Peper, Rüdel & Trautwein, 1967*a*, *b* Reuter, 1967). Nevertheless, there are good reasons for assuming that flow of K ions is the basis of slow outward current (Rougier *et al.*, 1968 Noble & Tsien, 1968, 1969*a*, *b*). As a first step, therefore, we should attemp to interpret the DNP-induced changes of membrane current in terms of a alteration of the fast Na- and the slow K-carrying system. Two simple ex planations are to be tested first. Since DNP is known to block the formatio of ATP in mitochondria, a breakdown of energy-dependent Na extrusio and K uptake through the cell membrane is to be expected. This will lea

to an increase of intracellular Na and a decrease of internal K, resulting in a shift of the equilibrium potentials E_{Na} and E_K towards zero and thereby changing the driving forces for passive ion movements. On the other hand, the membrane itself could be affected by an alteration of molecular structures controlling the Na and K permeability.

Concerning Na inward current, either explanation seems adequate. According to Fig. 6, there appears to be a shift of E_{Na} from +42 mV to about +20 mV after application of DNP. When the membrane potential is clamped at −20 mV, this shift in E_{Na} would mean a reduction of the driving force $(E-E_{Na})$ by about 1/3. This accounts only for a part of the strong depression of peak inward current actually observed. As a second factor, one can imagine an (incomplete) block of the Na channels caused by some reaction of DNP with critical sites of the cell membrane, similar to the block produced by quinidine, local anaesthetics, some alcohols, and other agents of different chemical structure (Weidmann, 1955; Narahashi, 1964). Both mechanisms proposed are consistent with the observation that the kinetics of the Na-carrying system (turn-on and turn-off of the transient current and recovery of peak inward current after a conditioning pulse) is not much affected by DNP. A block of Na channels would mean a reduction of $\overline{g_{Na}}$ in the Hodgkin-Huxley terminology (1952*b*).

Concerning the steady state current, an interpretation of the DNP effect is much more complicated. From the slight depolarization of the resting potential in the later stage of inhibition, one might expect only small changes in internal K concentration and K equilibrium potential (E_K). In any case, a shift of E_K from its normal value of about −73 mV (Haas, Glitsch & Kern, 1966) to more positive potentials tends to decrease K outward current at a given level of depolarization, in contrast to the strong increase experimentally observed. To interpret the augmented outward current in terms of a K mechanism, an increase of K membrane conductance $[g_K = I_K/(E-E_K)]$ must be assumed. According to Fig. 6, steady state current in DNP-Ringer's is four to five times the normal value at a given potential positive to −70 mV. Hence the increment in g_K would amount to 300 to 400% (or even more if a shift in E_K is accounted for). However, such a drastic increase in g_K is hard to reconcile with the observation that ^{42}K resting efflux increased by not more than 10 to 15% after application of DNP. The flux measurements were done at membrane potentials between about −65 and −55 mV so that an increased g_K should apply. There is little doubt that K efflux in normal frog atria is mainly a downhill process determined by the internal K concentration, the membrane potential, and the potassium permeability (P_K) of the membrane (Haas &

Glitsch, 1962; Haas *et al.*, 1966). In the constant-field theory of Goldman (1943) and Hodgkin and Katz (1949), the relation between P_K and g_K for membrane potentials near E_K is given by $P_K = g_K(RT)^2 (K_o - K_i)/F^3 E K_o K_i$. Thus, in spite of some uncertainty about the applicability of the Goldman theory to cardiac muscle, any large increment in g_K should be reflected by a similar increase of P_K and consequently of K efflux.

The conclusion from the discrepancy between voltage-clamp measurements and tracer experiments is that the increase in slow outward current is probably not due to an enhanced movement of K ions down their electrochemical gradient. Looking for another explanation, it is hard to name any other ion species as a candidate for an extra outward current induced by metabolic inhibition. In the first place, Cl or Ca ions are to be considered. In nerve, poisoning with DNP or cyanide causes a strong increase in intracellular free Ca. If such a rise occurs in cardiac tissue, this might lead to an extra outward current carried by Ca ions. However, because of the lack of any detailed information from flux measurements, this is no more than a speculative hypothesis.

An alternative idea is that an electrogenic pump could be involved in the potential, current and flux changes seen during exposure to DNP. The problem of active Na extrusion and K uptake has been studied most extensively in squid axons. The original idea of a one-for-one exchange of internal Na for external K (Hodgkin & Keynes, 1955*a*, *b*) probably requires some modification. Recent experiments (Baker, Blaustein, Hodgkin & Steinhardt, 1969; Baker, Blaustein, Keynes, Manil, Shaw & Steinhardt, 1969) suggest that the bulk of Na efflux occurs via the mechanism of a Na-K exchange with a Na-K ratio of about 2:1, and a small part of Na efflux may be coupled to Ca influx in a ratio of about 4:1. Thus both mechanisms seem inherently electrogenic. It is unknown to which extent these results can be applied to cardiac muscle. Flux measurements in frog atria using DNP, cyanide, Na-azide and ouabain as inhibitory agents (Haas *et al.*, 1967) revealed Na- and K-flux changes which differed from those seen in squid axon in many respects. A suspicious finding was that the ratio between DNP-sensitive Na efflux and K influx varied considerably when the external Na and K concentrations were changed (*see* Fig. 7 of Haas *et al.*, 1967). The Na-K ratio was 8:1 at $K_0 = 1.35$ mM, $Na_0 = 113$ mM, and 1:10 at $K_0 = 108$ mM, $Na_0 = 6$ mM. Even if the reservation is made that DNP may exert an influence on processes other than active transport, it is hard to believe that there should exist a common mechanism for Na and K transport with a fixed exchange ratio. A more plausible interpretation is that there is only a loose and variable coupling between Na and K transport

or no coupling at all, i.e., two transport systems acting independently. This would mean that Na and K transport occur to a large extent or even completely as a transfer of net charge across the membrane.

Thus it is tempting to use the concept of an electrogenic pump in interpreting the behavior of slow membrane current in our experiments. In the Appendix of this paper, a model of a carrier system transporting K ions uphill is explicitly calculated. The model is designed as a push-and-pull mechanism without affinity to ions other than K. Transport is regarded as a net K transfer composed of a carrier-mediated influx and efflux, the former exceeding the latter under normal conditions. The transport changes in magnitude and direction when the membrane potential is varied. With intact cell metabolism, the system has a reversal potential $E_{Tr} = +105$ mV, the transport being directed inward for $E < E_{Tr}$. A block of energy supply causes a shift of E_{Tr} towards E_K. If the block is complete, $E_{Tr} = E_K$. In this state the system performs a downhill transport at any membrane potential. In terms of thermodynamics, such a carrier-mediated downhill transport is indistinguishable from a free diffusion of K ions.

This model can explain the following findings:

(1) *The Decrease of K Resting Influx as Well as the Increase of K Efflux Observed after Application of DNP.* For a membrane potential of -63 mV (corresponding to the mean resting potential in frog atria), the model gives a reduction of carrier-mediated influx from 0.4 to 0.15 and an increase of carrier-mediated efflux from 0.04 to 0.17 (in relative units) after a complete inhibition. To refer these figures to the total fluxes, we assume that in normal frog atria carrier-mediated influx and efflux are 40% of total K influx (Haas *et al.*, 1967) and 4% of total K efflux, respectively. Thus we obtain a reduction of K resting influx by 25% and an increment in K efflux by 13%. This is in good agreement with the flux changes observed in the tracer experiments.

(2) *The Increase of Slow Outward Current Observed during Inhibition.* According to Figs. 8a, b and 11a, inhibition of the transport system induces an extra outward current at any membrane potential. This outward current equals the sum of a reduction in carrier-mediated K influx and an increment in K efflux. It is almost constant for membrane potentials between -100 and $+50$ mV. Its calculation is based upon the assumption that the diffusion coefficients of the carrier system (D for the electroneutral carrier-ion complex, D' for the free carrier anion) are constant values independent of the membrane potential. In voltage-clamp measurements, however, extra outward current was found to increase with the magnitude of depolarization

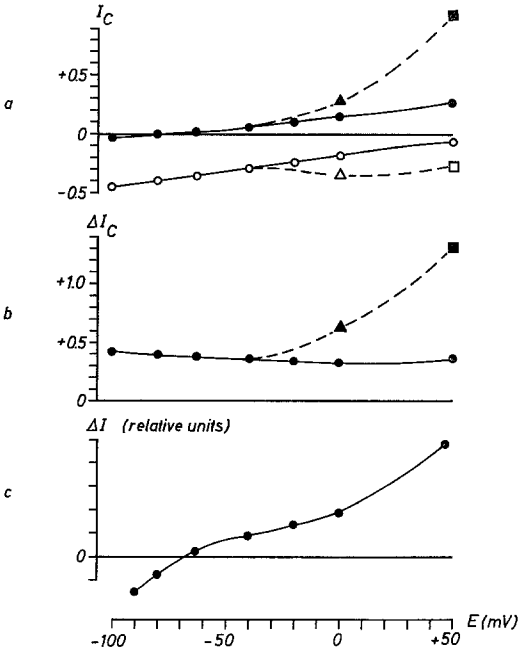

Fig. 8a–c. Comparison between theoretical and experimental steady state current-voltage relations. (a) Membrane current I_C carried by a hypothetical electrogenic K transport system before inhibition (open symbols) and after complete inhibition (filled symbols). The diffusion coefficient D' governing the movement of carrier anions through the membrane was taken as 10^{-13} (circles), 2.5×10^{-13} (triangles), and 10^{-12} cm^2/sec (squares). For details of the transport system, *see* Appendix. Note that outward current here has a positive sign, whereas in Fig. 11 outward current is denoted as negative. (b) Change in membrane current ΔI_C caused by inhibition of an electrogenic K transport system, calculated as the difference between the current-voltage relations in (a). Symbols as in (a). (c) DNP-induced change in steady state membrane current observed in voltage-clamp measurements. Values taken from Fig. 6. Membrane current is given in arbitrary units in all diagrams

(Figs. 6 & 8c). To adapt the model to the experimental results, the tentative hypothesis is made that the diffusion coefficient D' increases when the membrane is depolarized to potentials positive to -40 mV. This assumption seems not unreasonable since an increase of ionic permeability[1] owing to a depolarization is often encountered in case of ions penetrating the membrane, e.g., steady state K permeability in the squid axon (Hodgkin & Keynes, 1955*b*) and in the nodal membrane (Frankenhaeuser, 1962). As-

1 In the Goldman theory (1943), membrane permeability P is proportional to the diffusion coefficient of an ion species. For details, *see* Appendix.

suming an increase of D' by a factor of 2.5 and 10 at $E=0$ and $+50$ mV, respectively (with D being unchanged), a fair correspondence between the slope of the theoretical and the experimental current-voltage relation is obtained [Fig. 8b (broken line) and 8c] for membrane potentials between -40 and $+50$ mV.

An extra outward current caused by inhibition of K transport could also be the basis for the (transient) hyperpolarization of the resting potential seen in the beginning of the DNP period.

(3) *The Smallness of the DNP-Induced K Flux Changes (Expressed as Percentage) Compared to the Change in Outward Current.* The large increase in steady state outward current can be explained by assuming that in normal atria most of passive K outflow is cancelled by active inward transport so that a small change in the transport components is to cause a large change in net membrane current. A numerical example may illustrate this point. Suppose membrane current at $E=-40$ mV is mainly carried by K leakage and electrogenic K transport. According to Table 2 in the Appendix, carrier-mediated K influx and efflux at -40 mV change from 0.338 to 0.130 (in relative units) and from 0.044 to 0.191, respectively, owing to an inhibition. Influx and efflux related to free diffusion may be taken as 0.6 and 1.0, respectively [which is the same order as is found in resting preparations (Haas *et al.*, 1967)]. Assuming that the passive fluxes do not change during inhibition and calculating net flow as difference between efflux and influx, we obtain a passive outflow of $1.0-0.6=0.4$ which is reduced by an inward transport of $0.338-0.044=0.294$ to a net current of about 0.1 in normal atria and augmented by a downhill transport of $0.191-0.130=0.061$ to a net current of about 0.46 after inhibition. This means an increase in outward current by 360%. The corresponding K flux changes, however, are much smaller: total K influx decreases by $0.208/0.938=22\%$, and K efflux increases by $0.147/1.044=14\%$.

The foregoing analysis shows that the idea of an electrogenic inward transport renders a plausible interpretation of some membrane phenomena associated with a metabolic inhibition. Besides its merits, the model has an apparent defect: it predicts an extra steady state outward current at any membrane potential whereas an extra inward current was observed in hyperpolarizing clamps. However, the simple model used cannot be more than a first approach to the problem of electrogenic transport. A more complete theory should account for the transport of ions other than K. It seems possible that the extra inward current seen at hyperpolarized levels is caused by an inhibition of the Na pump.

Appendix

Model of an Electrogenic Pump

(H. G. Haas)

A model of active transport of ions across a membrane was designed for a mathematical analysis of the flux and current changes associated with a metabolic inhibition The main features of the model are as follows (Fig. 9).

The membrane is a homogeneous sheet interposed between two aqueous solutions containing the substrate S as a monovalent cation (S^+). Confined to the membrane there is a carrier C which can react with the substrate at the two membrane-solution interfaces. The free carrier is a monovalent anion (C^-), and the carrier-substrate complex (CS) is an electroneutral molecule. Carrier movement through the membrane is a diffusion process determined by the concentration gradient and the electric field within the membrane. The system operates as a cyclic mechanism: In order for an uphill transport to occur from side (1) to side (2), carrier and substrate react to form the complex at side (1); the complex then diffuses across the membrane to side (2) and breaks down; finally the free carrier diffuses back to side (1). Owing to the movement of the free carrier C^-, the pump is an electrogenic system. The reaction between carrier and substrate is linked to energy-yielding processes on one or both sides of the membrane The kinetic consequence of this coupling is an asymmetry of the rate constants governing the chemical reactions at the two interfaces. If the energy supply is blocked, the asymmetry of the rate constants diminishes gradually, approaching a state in which the rate constants are equal on both sides and correspond to the rate constants of the spontaneous reaction between carrier and substrate. In this state, the system will perform a passive downhill movement of the substrate rather than an active uphill transport.

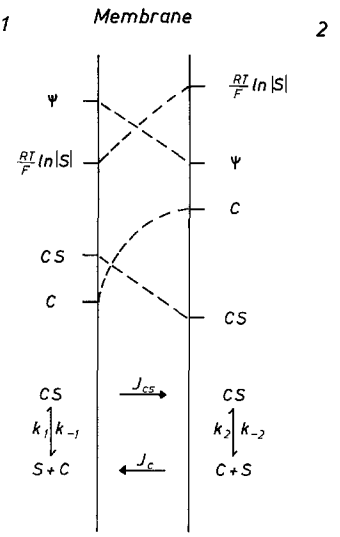

Fig. 9. Schematic diagram of a carrier system transporting ions uphill. *Top*: Gradients of the electrical and the chemical potential within the membrane. The resultant gradient is directed from side (2) to side (1). *Middle*: Concentration profiles of the free carrier (C) and the carrier-substrate complex (CS). *Bottom*: Reaction between carrier and substrate at the membrane-solution interfaces and carrier movement through the membrane

Table 1. *Symbols used*

Symbol	Meaning
1, 2	Subscripts related to the two sides of the membrane
d, δ	Thickness (cm) of the membrane and the boundary layers, respectively
C, S, CS	Free carrier, substrate, and carrier-substrate complex, respectively. In numerical equations, these symbols represent the respective concentrations (mole cm^{-3})
A	Total amount of carrier (mole cm^{-2})
k_1, k_2	Rate constants for association of carrier-substrate complex on the two sides of the membrane ($mole^{-1}\ cm^3\ sec^{-1}$)
k_{-1}, k_{-2}	Rate constants for dissociation of carrier-substrate complex (sec^{-1})
J_C, J_{CS}	Net flow of free carrier and carrier-substrate complex, respectively, across the membrane (mole $cm^{-2}\ sec^{-1}$). The flows are taken positive if directed from side (1) to side (2)
D', D	Diffusion coefficients ($cm^2\ sec^{-1}$) of the free carrier and the carrier-substrate complex, respectively
ψ	Electrical potential (mV) in the membrane phase
E	Membrane potential (mV) taken with respect to side (1)
E_{Tr}	Reversal potential (mV) of ion transport
F, R, T	Usual meanings
r	EF/RT
x	Linear coordinate (cm) vertical to the membrane
t	Time (sec)

The quantitative formulation starts from the processes on the two sides of the membrane. Association and dissociation of the carrier are assumed to occur within two narrow regions, the thickness (δ) of which is negligibly small compared to the thickness (d) of the bulk of the membrane. Combining the chemical reactions between carrier and substrate and the carrier flows, we obtain:

$$\frac{d(CS_1)}{dt} = k_1 S_1 C_1 - k_{-1}(CS_1) - J_{CS_1}/\delta, \tag{1a}$$

$$\frac{dC_1}{dt} = -k_1 S_1 C_1 + k_{-1}(CS_1) - J_{C_1}/\delta, \tag{1b}$$

$$\frac{d(CS_2)}{dt} = k_2 S_2 C_2 - k_{-2}(CS_2) + J_{CS_2}/\delta, \tag{1c}$$

$$\frac{dC_2}{dt} = -k_2 S_2 C_2 + k_{-2}(CS_2) + J_{C_2}/\delta \tag{1d}$$

where C_1, CS_1, S_1, etc., are the carrier and substrate concentrations in the δ-spaces, and J_{C_1}, etc., are the carrier flows at the boundaries between the δ-spaces and the bulk of the membrane. (The substrate concentrations S_1 and S_2 are, in general, not identical

with, but proportional to, those in the adjacent solutions, with the partition coefficien as the scale factor.) To give the Eqs. (1a–d) a definite meaning, it is necessary to establisl a correlation between the carrier flows within the membrane and the carrier concentra tions on the two sides. A general solution of this problem would require the integratio of partial differential equations related to the migration of CS and C^- in the membran phase, with Eqs. (1a–d) as the boundary conditions. In this paper we restrict the analysi to the steady state of the system. In this case the left sides of Eqs. (1a–d) vanish; th carrier flows J_C and J_{CS} are constant throughout the membrane and are equal bu opposite. Hence the system of the four Eqs. (1) reduces to two independent equation

$$k_1 S_1 C_1 - k_{-1}(CS_1) - J_{CS}/\delta = 0, \tag{2a}$$

and

$$k_2 S_2 C_2 - k_{-2}(CS_2) + J_{CS}/\delta = 0 \tag{2b}$$

with the subsidiary equation

$$J_{CS} = -J_C. \tag{2c}$$

A further relation follows from the conservation of carrier

$$\int_0^d (C + CS)\, dx = \text{const} = A \tag{2d}$$

where $x=0$ and $x=d$ correspond to side (1) and side (2), respectively.

To express J_{CS} and J_C in Eqs. (2a–c) in terms of the boundary carrier concentration and to evaluate the integral in Eq. (2d), we need concrete assumptions on the concen tration profiles of CS and C^-, respectively. Concerning the electroneutral complex CS we assume a linear concentration profile. Thus

$$J_{CS} = \frac{D}{d}(CS_1 - CS_2), \tag{3a}$$

and

$$\int_0^d CS\, dx = \frac{d}{2}(CS_1 + CS_2). \tag{3b}$$

Regarding the free carrier C^-, the shape of the concentration profile is essentiall dependent on the pattern of the electric field in the membrane. To keep the calculatio as simple as possible, we make use of the constant-field theory (Goldman, 1943). Ac cording to the relations of the Goldman theory, the concentration profile $C(x)$ is ex ponential

$$C(x) = C_1 + (C_2 - C_1)\frac{1 - e^{x\, r/d}}{1 - e^r} \tag{4a}$$

and

$$J_C = \frac{D' r}{d}\,\frac{C_2 - C_1 e^r}{1 - e^r}, \tag{4b}$$

$$\int_0^d C\, dx = d\left[\frac{C_2 - C_1 e^r}{1 - e^r} + \frac{C_2 - C_1}{r}\right], \tag{4c}$$

with $r = EF/RT$. By inserting the explicit terms of Eqs. (3a & b) and (4b & c) into Eqs. (2), we obtain a set of four equations for C_1, C_2, CS_1, and CS_2 which can be written

$$C_1(k_1 S_1) + CS_1\left(-k_{-1}-\frac{D}{d\delta}\right) + CS_2\left(\frac{D}{d\delta}\right) = 0, \tag{5a}$$

$$C_2(k_2 S_2) + CS_1\left(\frac{D}{d\delta}\right) + CS_2\left(-k_{-2}-\frac{D}{d\delta}\right) = 0, \tag{5b}$$

$$C_1(e^r) + C_2(-1) + CS_1\left(-\frac{D}{D'}\frac{1-e^r}{r}\right) + CS_2\left(\frac{D}{D'}\frac{1-e^r}{r}\right) = 0, \tag{5c}$$

$$C_1\left(\frac{-e^r}{1-e^r}-\frac{1}{r}\right) + C_2\left(\frac{1}{1-e^r}+\frac{1}{r}\right) + CS_1(0.5) + CS_2(0.5) = A/d. \tag{5d}$$

From these equations, the numerical values of C_1, C_2, CS_1, and CS_2 can be determined as functions of $S_1, S_2, k_1, k_{-1}, k_2, k_{-2}, D, D', d, \delta, r$, and A. The solution leads to rather complicated although mathematically simple terms. For the following we need the explicit values of CS_1 and CS_2:

$$CS_1 = \frac{-k_1 S_1 k_2 S_2 b_1 A/d}{a_1 b_2 - a_2 b_1}, \tag{6a}$$

and

$$CS_2 = \frac{k_1 S_1 k_2 S_2 a_1 A/d}{a_1 b_2 - a_2 b_1} \tag{6b}$$

with the abbreviations

$$a_1 = -\left(k_{-1}+\frac{D}{d\delta}\right)\frac{e^r}{k_1 S_1} + \frac{D}{D'}\frac{1-e^r}{r} - \frac{D}{d\delta}\frac{1}{k_2 S_2},$$

$$b_1 = \frac{D}{d\delta}\frac{e^r}{k_1 S_1} - \frac{D}{D'}\frac{1-e^r}{r} + \left(k_{-2}+\frac{D}{d\delta}\right)\frac{1}{k_2 S_2},$$

$$a_2 = \left[\frac{k_1 S_1}{2} - \left(k_{-1}+\frac{D}{d\delta}\right)\left(\frac{e^r}{1-e^r}+\frac{1}{r}\right)\right] k_2 S_2 - \frac{D}{d\delta}\left(\frac{1}{1-e^r}+\frac{1}{r}\right) k_1 S_1,$$

$$b_2 = \left[\frac{k_1 S_1}{2} + \frac{D}{d\delta}\left(\frac{e^r}{1-e^r}+\frac{1}{r}\right)\right] k_2 S_2 + \left(k_{-2}+\frac{D}{d\delta}\right)\left(\frac{1}{1-e^r}+\frac{1}{r}\right) k_1 S_1.$$

An important relation following from Eqs. (6a & b) is

$$\frac{CS_1}{CS_2}=\frac{+b_1}{-a_1}=\frac{\frac{D}{d\delta}\frac{e^r}{k_1 S_1}-\frac{D}{D'}\frac{1-e^r}{r}+\left(k_{-2}+\frac{D}{d\delta}\right)\frac{1}{k_2 S_2}}{\left(k_{-1}+\frac{D}{d\delta}\right)\frac{e^r}{k_1 S_1}-\frac{D}{D'}\frac{1-e^r}{r}+\frac{D}{d\delta}\frac{1}{k_2 S_2}}. \tag{7}$$

From this relation, the kinetical condition for an uphill transport is clearly seen. Suppose the gradient of the electrochemical potential of S^+ is directed from side (2) to side (1) so that $(E-E_S)>0$, E_S being the equilibrium potential for a passive diffusion of the free ion S^+ calculated from the Nernst equation

$$E_S=\frac{RT}{F}\ln S_1/S_2\,. \tag{8}$$

An uphill transport from side (1) to side (2) requires the relation $CS_1>CS_2$ which is equivalent to $\frac{k_{-2}}{k_2 S_2}>e^r\frac{k_{-1}}{k_1 S_1}$ or

$$\frac{k_1 k_{-2}}{k_{-1} k_2}>e^r\frac{S_2}{S_1}=e^{(E-E_S)F/RT}>1. \tag{9}$$

This is the quantitative formulation of the asymmetry of the rate constants which is necessary for an uphill transport. A simple interpretation is that there must be a high value of k_1 and a low value of k_{-1} in order for the association of the carrier-substrate complex to exceed the dissociation on side (1), and a low value of k_2 and a high value of k_{-2} for the dissociation to prevail on side (2). Correspondingly, the condition for a downhill transport is

$$CS_1<CS_2 \quad \text{or} \quad \frac{k_1 k_{-2}}{k_{-1} k_2}<e^{(E-E_S)F/RT}>1. \tag{10}$$

This condition is satisfied, for example, in the case that the reaction between carrier and substrate occurs spontaneously on both sides of the membrane and thus $k_1=k_2$, $k_{-1}=k_{-2}$.

It is instructive to put these results in a generalized form. Obviously the relations

$$CS_1>CS_2 \quad \text{or} \quad \frac{k_1 k_{-2}}{k_{-1} k_2}>e^{(E-E_S)F/RT} \tag{11a}$$

and

$$CS_1<CS_2 \quad \text{or} \quad \frac{k_1 k_{-2}}{k_{-1} k_2}<e^{(E-E_S)F/RT} \tag{11b}$$

are the conditions for any transport from side (1) to side (2) and from (2) to (1), respectively, no matter what the sign of $(E-E_S)$ is. If the concentrations S_1 and S_2 and the rate constants k_1, k_{-1}, k_2, and k_{-2} are given values and the membrane potential is regarded as a variable, Eqs. (11a & b) may be solved for E. Thus we have

$$E\lessgtr\frac{RT}{F}\ln\frac{S_1}{S_2}\frac{k_1 k_{-2}}{k_{-1} k_2} \tag{12}$$

as the condition for a transport from side (1) to side (2) and vice versa, respectively (the symbol $<$ being related to the first case). In other words, the transport system has a reversal potential

$$E_{\mathrm{Tr}}=\frac{RT}{F}\ln\frac{S_1}{S_2}\frac{k_1 k_{-2}}{k_{-1}k_2}=E_S+\frac{RT}{F}\ln\frac{k_1 k_{-2}}{k_{-1}k_2}. \tag{13}$$

This is a modification of the Nernst equation. It clearly demonstrates the importance of the asymmetry of the rate constants. The greater this asymmetry, the larger is the difference between E_{Tr} and E_S. Fig. 10a illustrates the meaning of this point. At any membrane potential between E_{Tr} and E_S, active transport (in the form of the complex CS) is opposite to passive diffusion of the free cation S^+ through the membrane. It is only in this range of membrane potential that the carrier system performs an uphill transport. In the other ranges of membrane potential, active transport and passive diffusion are in parallel. In that case, active transport goes downhill and may be regarded as "facilitated diffusion".

At this stage it seems reasonable to clarify how an asymmetry of the rate constants is brought about. For simplicity we consider the case that the reaction $C+S\rightleftharpoons CS$ occurs in a closed system and has reached equilibrium. (This is somewhat different from the situation in our model where the δ-spaces are open systems and the reaction $C+S\rightleftharpoons CS$ is close to, but not at, equilibrium. However, this difference does not affect the following consideration.) If the reaction occurs spontaneously, the equilibrium is characterized, from a thermodynamic point of view, by

$$\varphi_C+\varphi_S-\varphi_{CS}=0, \tag{14}$$

the φ's being the respective chemical potentials of the reactants. (In the case of a dilute solution, φ_C is given by $RT\ln|C|+\mathrm{const}$, and similarly the other potentials.) If the formation of the carrier-substrate complex $C+S\rightarrow CS$ is coupled to an exergonic reaction, say $P\rightarrow Q$, the overall reaction is $C+S+P\rightleftharpoons CS+Q$ and equilibrium is given by

$$\varphi_C+\varphi_S+\varphi_P-\varphi_{CS}-\varphi_Q=0. \tag{15}$$

Since $\varphi_P-\varphi_Q>0$, it follows for the carrier-substrate reaction

$$\varphi_C+\varphi_S-\varphi_{CS}<0. \tag{16}$$

Provided the total carrier concentration $C+CS$ and the total substrate concentration $S+CS$ is the same in both cases, relation (16) means that in the case of the coupled reaction the equilibrium between C, S and CS is shifted to lower concentrations of C and S and to a higher concentration of CS compared with the spontaneous reaction. In terms of the rate constants of the reaction $C+S\underset{k_-}{\overset{k}{\rightleftharpoons}}CS$, this shift is equivalent to an increase of k and a decrease of k_-. (Generally speaking, the ratio k/k_- has changed to a higher value.) Conversely, if not the formation but the breakdown of the carrier-substrate complex is linked to an energy-delivering reaction, we obtain a decreased value of k and an increased value of k_-. By applying these results to the model and recalling the interpretation of Eq. (9), it is easy to verify that an uphill transport requires the coupling of an energy-delivering process either to the formation of the carrier-substrate complex on the downhill side ("push-mechanism") or to the breakdown of the complex on the uphill side ("pull-mechanism") or to both reactions ("push-and-pull-mechanism").

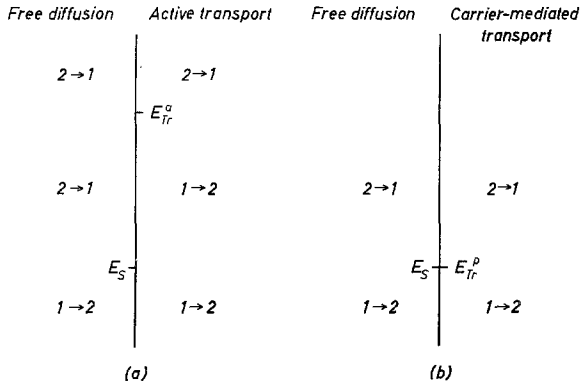

Fig. 10a and b. Direction of carrier-mediated transport and free diffusion of a cation S^+ across a membrane in various regions of the membrane potential in the active state (a) and in the passive state (b) of the transport system. The vertical axis is a scale of membrane potential (increasing upwards). E^a_{Tr} and E^p_{Tr} are the respective reversal potentials of the system in the active and the passive state. E_S is the equilibrium potential for free diffusion of S^+

Now that the general kinetics and energetics of the model have been worked out, the influence of an inhibition on the transport system can be demonstrated easily. We start from an "active" state of the system with a continuous energy input from exergonic metabolic reactions. This situation is characterized by an appropriate asymmetry of the rate constants governing the reaction between carrier and substrate on the two sides of the membrane and by a transport equilibrium potential E^a_{Tr}[2] which is different from the equilibrium potential E_S of the free diffusion of the cation S^+ [*see* Eq. (13) and Fig. 10a]. Uphill transport is restricted to the range of membrane potential between E^a_{Tr} and E_S. If the energy supply is blocked by metabolic inhibitors or by other suitable changes, the asymmetry of the rate constants will diminish gradually. After inhibition is completed, the rate constants are symmetrical on both sides of the membrane and equal to those of the spontaneous reaction. In terms of the transport equilibrium potential, the loss of asymmetry of the rate constants means a shift of E_{Tr} towards E_S. The "passive" state finally reached is characterized by $E^p_{Tr}{}^2 = E_S$. The carrier system now performs a transport of S which is in parallel to the free diffusion on S^+ and thus a downhill movement at any membrane potential (Fig. 10b).

The effect of an inhibition on the carrier flows can best be seen for membrane potentials between E^a_{Tr} and E_S. In this potential range, steady state flow J_{CS} changes its direction: it goes uphill before inhibition and downhill after inhibition. At any potential outside this range, the direction of J_{CS} remains unchanged and only the magnitude will change owing to an inhibition. The membrane current associated with the transport is the flow of the free carrier J_C. Since $J_{CS} = -J_C$ in the steady state, any change in J_{CS} is coupled with a corresponding change in J_C and equivalent to an extra current through the membrane.

A more detailed interpretation of the effect of an inhibition is obtained if the unidirectional fluxes rather than the net flows of the carrier system are taken into account. The carrier flows as defined by Eqs. (3a) and (4b) can be separated into two components, each of which is proportional to the carrier concentration on one side of the membrane

2 The superscripts a and p refer to the active and the passive state, respectively.

and can be regarded as a unidirectional flux directed from this side to the other:

$$M_{CS}^{12}=\frac{D}{d}CS_1, \qquad M_{CS}^{21}=\frac{D}{d}CS_2, \tag{17a, b}$$

$$M_{C}^{12}=\frac{-D'r}{d}\frac{C_1 e^r}{1-e^r}, \qquad M_{C}^{21}=\frac{-D'r}{d}\frac{C_2}{1-e^r}. \tag{17c, d}$$

A change in the carrier net flows caused by an inhibition is reflected by an appropriate change in the unidirectional carrier fluxes. However, one has to keep in mind that a given change in net flow may be realized by a variety of changes in the unidirectional fluxes. For example, if the *CS* flow changes its direction from uphill to downhill, this net change may be brought about by (1) an increase of the downhill component, the uphill component being unchanged; (2) a decrease of the uphill component, the downhill component being unchanged; (3) an increase of the downhill component and a decrease of the uphill component; (4) an increase of the downhill component and a (smaller) increase of the uphill component; or (5) a decrease of the downhill component and a (larger) decrease of the uphill component.

Which of these five cases will occur cannot be predicted without a detailed knowledge of the parameters of the system. In the first place, the flux changes will depend on the site of the block. The primary effect of an inhibition is to alter the carrier concentrations on that side of the membrane where the reaction between carrier and substrate is linked to metabolism. This leads to a change in the carrier fluxes going from this side to the other. Concerning the *CS* fluxes, this means an increased downhill flux in the case of a pull-mechanism, a decreased uphill flux in the case of a push-mechanism, and a combination of both in the case of a push-and-pull-mechanism. This statement corresponds to that given by Rosenberg and Wilbrandt (1963) in their treatment of a carrier system transporting an electroneutral substrate.

A concrete example may be useful to illustrate the effect of an inhibition on an electrogenic pump. Suppose K transport across the cell membrane is carried out by a system of the type described above. We identify side (1) of the model with the outside of the cell membrane. To match the situation in frog atria, we assume a resting potential of -63 mV ($r=-2.5$) and a ratio between extracellular and intracellular K concentration of 1:18 (Haas *et al.*, 1966), corresponding to an equilibrium potential

$$E_K=\frac{RT}{F}\ln\frac{1}{18}=-73\text{ mV}.$$

The thicknesses of the cell membrane and of the boundary layers are taken as $d=0.7\times10^{-6}$ cm and $\delta=0.03\times10^{-6}$ cm, respectively. The diffusion coefficients of the carrier-substrate complex and the free carrier are assumed to be $D=10^{-12}$ and $D'=10^{-13}$ cm^2 sec^{-1}, respectively. This is the same order of magnitude as is found for the free diffusion of K ions across the cell membrane[3].

3 Using the relations of the constant-field theory (Goldman, 1943), the diffusion coefficient D is related to the membrane permeability P of an ion species by $D=Pd/\beta$ where d is the thickness of the membrane and β the partition coefficient between membrane and adjacent medium. Values experimentally found for P_K in the resting state are between 10^{-6} and 10^{-7} cm sec^{-1} (Haas, 1964). If β is assumed to be in the order of 1 and d is taken as about 100 A, a value of D_K between 10^{-12} and 10^{-13} cm^2 sec^{-1} is obtained for the free diffusion of K ions through the membrane.

Table 2. *Carrier concentrations*[a] *at various membrane potentials*

E (mV)	Before inhibition				After inhibition			
	C_1	C_2	CS_1	CS_2	C_1	C_2	CS_1	CS_2
−100	0.355	1.170	0.501	0.037	3.96	0.172	0.196	0.157
−80	0.298	1.241	0.446	0.038	3.47	0.179	0.173	0.162
−63	0.267	1.348	0.400	0.040	3.03	0.190	0.152	0.170
−40	0.225	1.521	0.338	0.044	2.53	0.215	0.130	0.191
−20	0.189	1.729	0.286	0.048	2.15	0.248	0.113	0.218
0	0.158	2.012	0.240	0.055	1.85	0.288	0.099	0.252
+50	0.097	3.049	0.153	0.079	1.324	0.423	0.08	0.368
+105	0.07	4.68	0.117	0.117	1.04	0.59	0.07	0.51

[a] Carrier concentrations are given in relative units. For details of the transpor system *see* text.

The situation before inhibition (the active state of the system) may be characterizec as follows. Suppose K inward transport in resting preparations is composed of a large CK influx and a small CK efflux, with a flux ratio of 10:1. According to Eqs. (17a & b) the same ratio applies to the steady state carrier concentrations CK_1 and CK_2. For simplicity, the K concentrations on the two sides of the membrane are denoted by $K_1=1$ and $K_2=18$, respectively, and all carrier concentrations are given with respect to K_1. A set of rate constants and carrier concentrations which satisfies the condition $CK_1:CK_2=10:1$ and the Eqs. (5a–c) at $E=-63$ mV is

$$CK_1=0.4 \qquad C_1=0.267 \qquad CK_2=0.04 \qquad C_2=1.348$$
$$k_1=643 \qquad k_2=4.56 \qquad \text{(unit of concentration)}^{-1}\,\text{sec}^{-1}$$
$$k_{-1}=386 \qquad k_{-2}=3{,}192 \qquad \text{sec}^{-1}.$$

Inserting these values in Eq. (5d) gives a mean total carrier concentration $A/d=1.232$. The choice of the rate constants is, of course, arbitrary because of the lack of any evidence on the chemical nature of the membrane carrier, but the numerical values are not unreasonable when compared with those normally encountered in organic chemistry. The values given above lead to a transport equilibrium potential

$$E_{Tr}=E_K+\frac{RT}{F}\ln\frac{k_1 k_{-2}}{k_{-1} k_2}=-73+178=+105\,\text{mV}.$$

This means that K transport goes uphill in the whole potential range between the resting value and the peak of the action potential. If the diffusion coefficients, the rate constants, the total amount of carrier, and the K concentrations K_1 and K_2 are regarded as constants, the carrier concentrations C_1, C_2, CK_1, and CK_2 (and consequently the carrier flows and fluxes) at any membrane potential other than the resting value can be determined by solving Eqs. (5a–d). Numerical values of carrier concentrations for membrane potentials between −100 and +105 mV are given on the left in Table 2.

To demonstrate the effect of an inhibition, we assume that K inward transport is based on a push-and-pull-mechanism (with a link to energy-yielding reactions on both sides of the membrane) and that after a complete block of energy input (in the passive

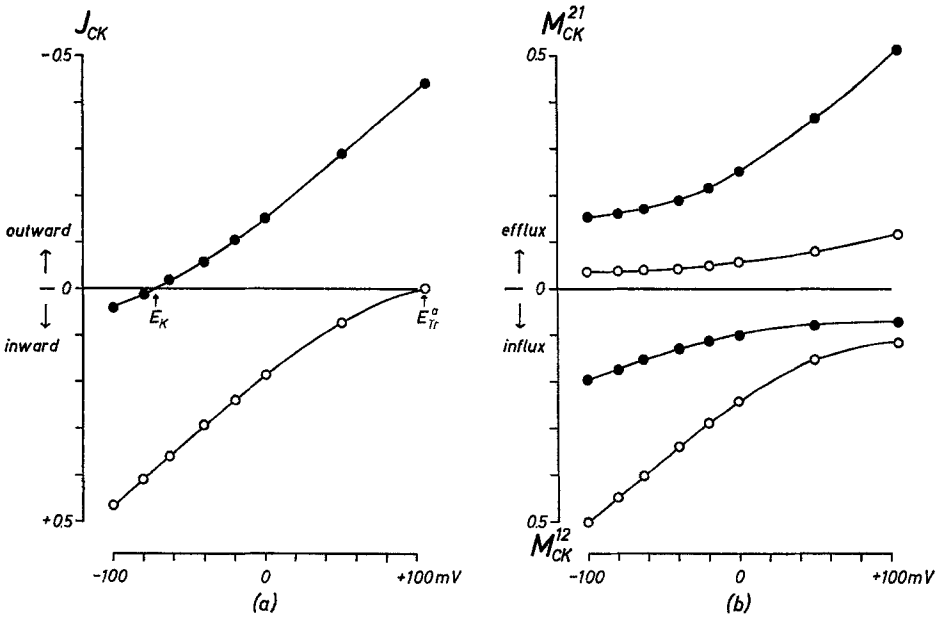

Fig. 11. (a) Carrier net flow J_{CK} and (b) carrier influx M_{CK}^{12} and efflux M_{CK}^{21} of an electrogenic K pump as a function of membrane potential. The parameters of the system are given in the text. Net flow, influx, and efflux are taken as $(CK_1 - CK_2)$, CK_1, and CK_2, respectively (*see* Table 2), the factor D/d being omitted. The open circles represent the active state of the system, the filled circles represent the passive state (after complete inhibition)

state) the rate constants have changed to

$$k_1 = k_2 = 50 \quad \text{(unit of concentration)}^{-1}\,\text{sec}^{-1}$$

$$k_{-1} = k_{-2} = 1{,}000 \quad \text{sec}^{-1}.$$

Again the steady state values of the carrier concentrations at any membrane potential are obtained by solving Eqs. 2 (a–d). Results are summarized on the right in Table 2.

K net transport and its unidirectional components are calculated from Eqs. (3a) and (17a & b). Fig. 11a shows the net flow J_{CK} as a function of membrane potential, i.e., the current-voltage relation of the transport system for both the active and the passive state. (Note that a positive sign of J_{CK} means an inward current, in contrast to the terminology normally used in electrophysiology.) The system exhibits an anomalous (inward-going) rectification in the active state and a normal (outward-going) rectification in the passive state. The flow change caused by the inhibition is equivalent to an extra outward current over the whole range of membrane potential. The unidirectional CK fluxes are shown in Fig. 11b. The effect of the inhibition is, roughly speaking, a two- to threefold reduction of CK influx and a four- to fivefold enhancement of CK efflux. Both the decrement in influx and the increment in efflux contribute to the extra outward current.

We wish to express our gratitude to Prof. John W. Moore for valuable advice o the experimental arrangement and to Dr. M. Tarr for helpful collaboration in preparin the manuscript.

This investigation was supported by the Deutsche Forschungsgemeinschaft and th Stiftung Volkswagenwerk.

References

Bak, A. F. 1958. A unity gain cathode follower. *Electroenceph. Clin. Neurophysiol.* **10**:74
Baker, P. F., Blaustein, M. P., Hodgkin, A. L., Steinhardt, R. A. 1969. The influenc of calcium on sodium efflux in squid axons. *J. Physiol.* **200**:431.
— —, Keynes, R. D., Manil, J., Shaw, T. I., Steinhardt, R. A. 1969. The ouabain sensitive fluxes of sodium and potassium in squid giant axons. *J. Physiol.* **200**:45
Beeler, G. W., Reuter, H. 1970. Voltage clamp experiments on ventricular myocardia fibres. *J. Physiol.* **207**:165.
Blaustein, M. P., Goldman, D. E. 1966. Origin of axon membrane hyperpolarizatio under sucrose-gap. *Biophys. J.* **6**:453.
Brady, A. J., Woodbury, J. W. 1951. Effects of sodium and potassium on repolarizatio in frog ventricular fibers. *Ann. N.Y. Acad. Sci.* **65**:687.
Deck, K. A., Trautwein, W. 1964. Ionic currents in cardiac excitation. *Pflüg. Arch. Ge Physiol.* **280**:63.
Dudel, J., Peper, K., Rüdel, R., Trautwein, W. 1967*a*. The dynamic chloride componen of membrane current in Purkinje fibers. *Pflüg. Arch. Ges. Physiol.* **295**:197.
— — — — 1967*b*. The effect of tetrodotoxin on the membrane current in cardia muscle (Purkinje fibers). *Pflüg. Arch. Ges. Physiol.* **295**:213.
Frankenhaeuser, B. 1962. Potassium permeability in myelinated nerve fibres of *Xenopu laevis*. *J. Physiol.* **160**:54.
Goldman, D. E. 1943. Potential, impedance, and rectification in membranes. *J. Ge Physiol.* **27**:37.
Haas, H. G. 1964. Ein Vergleich zwischen Fluxmessungen und elektrischen Messunge am Myokard. *Pflüg. Arch. Ges. Physiol.* **281**:271.
— Glitsch, H. G. 1962. Kalium-Fluxe am Vorhof des Froschherzens. *Pflüg. Arch. Ge Physiol.* **275**:358.
— — Kern, R. 1966. Kalium-Fluxe und Membranpotential am Froschvorhof in Ab hängigkeit von der Kalium-Außenkonzentration. *Pflüg. Arch. Ges. Physiol.* **288**:4
— — Trautwein, W. 1963. Natrium-Fluxe am Vorhof des Froschherzens. *Pflüg. Arc Ges. Physiol.* **277**:36.
—, Hantsch, F., Otter, H. P., Siegel, G. 1967. Untersuchungen zum Problem des aktive K- und Na-Transports am Myokard. *Pflüg. Arch. Ges. Physiol.* **294**:144.
Hodgkin, A. L., Huxley, A. F. 1952*a*. The dual effect of membrane potential on sodiu conductance in the giant axon of Loligo. *J. Physiol.* **116**:497.
— — 1952*b*. A quantitative description of membrane current and its application t conduction and excitation in nerve. *J. Physiol.* **117**:500.
— Katz, B. 1949. The effect of sodium ions on the electrical activity of the giant axo of the squid. *J. Physiol.* **108**:37.
— Keynes, R. D. 1955*a*. Active transport of cations in giant axons from Sepia an Loligo. *J. Physiol.* **128**:28.
— — 1955*b*. The potassium permeability of a giant nerve fibre. *J. Physiol.* **128**:6
Julian, F. J., Moore, J. W., Goldman, D. E. 1962*a*. Membrane potentials of the lobst giant axon obtained by use of the sucrose-gap technique. *J. Gen. Physiol.* **45**:119
— — — 1962*b*. Current-voltage relations in the lobster giant axon membrane und voltage clamp conditions. *J. Gen. Physiol.* **45**:1217.

Kleinfeld, M., Magin, J., Stein, E. 1961. Effect of 2,4-dinitrophenol on electrical and mechanical activities of isolated heart. *Amer. J. Physiol.* **201**:467.

Lüllmann, H. 1959. Das Verhalten der cellulären Potentiale der Herzmuskulatur bei verschiedenen experimentellen „Insuffizienzformen". *Arch. Exp. Pathol. Pharmakol.* **237**:447.

Macfarlane, W. V. 1960. The plateau of the action potential of the frog ventricle. *Circulation Res.* **8**:47.

Narahashi, T. 1964. Restoration of action potential by anodal polarization in lobster giant axons. *J. Cell. Comp. Physiol.* **64**:73.

— Moore, J. W., Scott, W. R. 1964. Tetrodotoxin blockage of sodium conductance increase in lobster giant axons. *J. Gen. Physiol.* **47**:965.

Noble, D., Tsien, R. W. 1968. The kinetics and rectifier properties of the slow potassium current in cardiac Purkinje fibres. *J. Physiol.* **195**:185.

— — 1969*a*. Outward membrane currents activated in the plateau range of potentials in cardiac Purkinje fibres. *J. Physiol.* **200**:205.

— — 1969*b*. Reconstruction of the repolarization process in cardiac Purkinje fibres based on voltage clamp measurements of membrane current. *J. Physiol.* **200**:233.

Reuter, H. 1967. The dependence of slow inward current in Purkinje fibres on the extracellular calcium-concentration. *J. Physiol.* **192**:479.

Rosenberg, T., Wilbrandt, W. 1963. Carrier transport uphill. I. General. *J. Theoret. Biol.* **5**:288.

Rougier, O., Vassort, G., Garnier, D., Gargouil, Y. M., Coraboeuf, E. 1969. Existence and role of a slow inward current during the frog atrial action potential. *Pflüg. Arch. Ges. Physiol.* **308**:91.

— — Stämpfli, R. 1968. Voltage clamp experiments on frog atrial heart muscle fibres with the sucrose-gap technique. *Pflüg. Arch. Ges. Physiol.* **301**:91.

Stämpfli, R. 1963. Die doppelte Saccharosetrennwandmethode zur Messung von elektrischen Membraneigenschaften mit extracellulären Elektroden. *Helv. Physiol. Acta* **21**:189.

Trautwein, W., Dudel, J. 1956. Aktionspotential und Kontraktion des Herzmuskels im Sauerstoffmangel. *Pflüg. Arch. Ges. Physiol.* **263**:23.

— — Peper, K. 1965. Stationary S-shaped current voltage relation and hysteresis in heart muscle fibres. Excitatory phenomena in Na^+-free bathing solutions. *J. Cell. Comp. Physiol.* **66**:79.

Webb, J. L., Hollander, P. B. 1956. Metabolic aspects of the relationship between the contractility and membrane potentials of the rat atrium. *Circulation Res.* **4**:618.

Weidmann, S. 1955. Effects of calcium ions and local anaesthetics on electrical properties of Purkinje fibres. *J. Physiol.* **129**:568.